Molecular Crystals and Liquid Crystals

Publication details, including instructions for authors and subscription information:
http://www.tandfonline.com/loi/gmcl20

Photorefractive Polymer Composites based on Third-Order Nonlinear Optical Chromophores

L. Ya. Pereshivko [a], A. D. Grishina [a], T. V. Krivenko [a], V. V. Savelev [a] & A. V. Vannikov [a]

[a] A.N. Frumkin Institute of Physical Chemistry and Electrochemistry, Russian Academy of Sciences, Moscow, Russia

Version of record first published: 06 Jul 2012

To cite this article: L. Ya. Pereshivko, A. D. Grishina, T. V. Krivenko, V. V. Savelev & A. V. Vannikov (2008): Photorefractive Polymer Composites based on Third-Order Nonlinear Optical Chromophores, Molecular Crystals and Liquid Crystals, 496:1, 293-301

To link to this article: http://dx.doi.org/10.1080/15421400802451881

Mol. Cryst. Liq. Cryst., Vol. 496, pp. 293–301, 2008

ISSN: 1542-1406 print/1563-5287 online
DOI: 10.1080/15421400802451881

Taylor & Francis
Taylor & Francis Group

Photorefractive Polymer Composites based on Third-Order Nonlinear Optical Chromophores

L. Ya. Pereshivko, A. D. Grishina, T. V. Krivenko, V. V. Savelev, and A. V. Vannikov
A.N. Frumkin Institute of Physical Chemistry and Electrochemistry, Russian Academy of Sciences, Moscow, Russia

Photorefractive materials based on unplasticized polymers that have a high glass transition temperature and the frozen random orientation of chromophores are prepared by layer casting. Under these conditions, only the third-order susceptibility has a nonzero value, by increasing with an increase in the conjugation chain length and reaching considerable values in the case of nano-sized molecules, such as single wall carbon nanotubes. In single wall carbon nanotubes containing poly-N-vinylcarbazole, the photoelectric sensitivity and photorefractive characteristics are measured at 1064 and 1550 nm.

Keywords: carbon nanotubes; photoconductivity; photorefractive polymers

INTRODUCTION

The capability to amplify IR laser beams makes photorefractive materials promising for optical diagnostics in medicine (1064 nm) and in optical communication processes (1550 nm). Therefore, the development of devices for the enhancement of informative laser beams in this range is an important problem.

The photorefractive (PR) effect is known to be characteristic of polymer materials that possess photoelectric, charge transport, and nonlinear optical properties. The PR effect includes the following processes (Fig. 1): interference of two input laser beams, photogeneration

We are grateful to R.W. Rychwalski and L. Licea-Jiménez (Chalmers University of Technology, Sweden) for providing single wall carbon nanotubes. This work was supported by the ISTC (No. 3718) and RFBR (Project 08-03-00125 and 07-03-13547).

Address correspondence to L. Ya. Pereshivko, A. N. Frumkin Institute of Physical Chemistry and Electrochemistry, Russian Academy of Sciences, 31, Leninsky pr., Moscow, 119991, Russia. E-mail: pereshivko@elchem.ac.ru

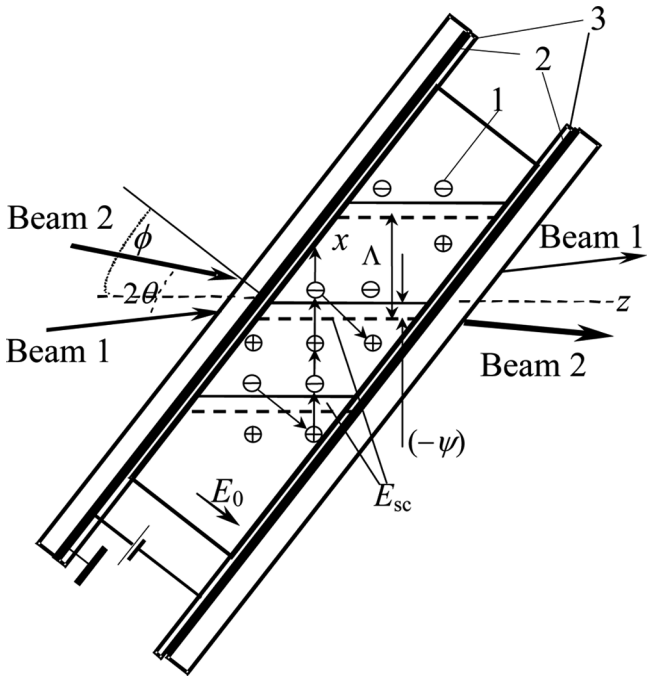

FIGURE 1 Schematic representing the interaction geometry of the writing beams 1 and 2 with a polymer composite: composite layer (1), ITO-electrodes (2), Al_2O_3–insulating barrier (3). The sample is titled at $\phi = 45^\circ$, the angle between beams is $2\theta = 15^\circ$. E_0 is the applied electric field. Solid and dashed lines inside the composite layer denote the interference and diffraction gratings, resapectively. Electrons are trapped near bright bands, holes drift to dark regions. The periodic field E_{sc} is directed along the x-axis, Λ is the grating period, $\psi = 2\pi\Delta x/\Lambda$ and Δx are the phase and spatial shifts between the gratings, respectively.

of electron-hole pairs in the bright interference bands (Fig. 1, solid lines in the polymer layer), and the prevailing drift of one of the charges, as an example, of the holes in the direction of the applied electric field E_0 to the dark regions (the plus and minus signs represent trapped holes and electrons, respectively). The periodic space charge field E_{sc} is formed as a result of the trapping of both electrons and holes along dark regions. The orientation of dipole molecules and the electron polarizability of chromophores in the periodic field E_{sc} provide the modulation of the refractive index Δn and the diffraction grating formation, which is shifted in space relative to the bright fringes

(dashed lines in Fig. 1). A necessary condition for the emergence of the PR effect is a difference in the mobilities of unlike charges. Seeing the drift of electrons in the direction opposite to that of holes, this electron displacement limits the phase shift ψ (Fig. 1) and decreases the beam-coupling gain coefficient:

$$\Gamma = 4\pi\ \Delta n \cos 2\theta \sin \psi/\lambda. \tag{1}$$

For the geometry of the sample shown in Figure 1, the field E_{sc} and, hence, Δn peaks are spatially shifted relative to the interference bands by the distance $-\Delta x$ or by the phase $-\psi = 2\pi(-\Delta x)/\Lambda$, where Λ is the grating spacing.

As a consequence, beam 1 (pump) reflected from the grating travels parallel to and is in phase with beam 2 (signal), and their interference provides the amplification of the signal beam. The reflected beam 2 is out of phase with beam 1, and the intensity of the latter decreases due to their interference (Fig. 1).

The vast majority of PR materials were synthesized using plasticized polymer composites with glass transition temperatures (T_g) close to room temperature [1–4]. In these polymers, the high diffusive mobility of low-molecular dipolar chromophores is responsible for their orientation in the direction of E_{sc}. In this case, the index refraction modulation is provided by two contributions: the orientation polarization and the second-order polarization. Polymers with low T_g have high PR characteristics, but the high diffusive mobility of chromophores leads to a short lifetime of stable PR composites due to the dimerization or crystallization of chromophores. Therefore, there is a strong need for the PR polymers with a high T_g and high PR characteristics.

The main purpose of our work is the creation of PR materials based on a polymer having a high T_g. This task requires to use third-order nonlinear optical chromophores. The chaotic distribution of chromophores is "frozen" in the stiff polymers having high T_g. In this case, the orientation polarization and the second-order polarization equal zero, and only the third-order susceptibility has non-zero value, increasing with the conjugation chain length and reaching considerable values in the case of nano-sized molecules, such as single wall carbon nanotubes. Poly-N-vinylcarbazole was used as the polymer matrix ($T_g = 200^{\circ}C$).

The electron polarizability reacts to a change of E_{sc} on the timescale of picoseconds. Therefore, the PR properties are determined by the photogeneration quantum efficiency, the mobility of charge carriers, and their dependence on an applied electric field.

EXPERIMENTAL

The PR composites consist of poly-N-vinylcarbazole (PVK) and 0.26 wt.% oxidized single wall carbon nanotubes (o-SWCNT) or 0.26 wt.% non-oxidized single wall carbon nanotubes (SWCNT). PVK as-received from Aldrich was used. SWCNT material (AP-grade) produced by an arc discharge was purchased from CarboLex (USA). According to the manufacturer, the purity was 50–70 vol.% as determined by Raman spectroscopy and SEM. Impurities included approximately 35 wt.% of residual catalyst particles (Ni, Y), and some amorphous carbon might also be present. SWCNT had an average diameter of 1.4 nm, and their samples include both semiconducting (2/3) and metallic (1/3) tubes with chiral angles distributed between 0° and 30°. SWCNT were purified for the removal of impurities by treating in 65% nitric acid for 26 h. Then, after filtering off, SWCNT were washed several times with deionized water on a centrifuge until pH7. o-SWCNT were obtained by means of the treatment of SWCNT in aquafortis at 110–120°C in the course of 24 h.

To prepare composites, SWCNT were first dispersed in tetrachloroethane for 30 min by an UZDN-A ultrasonic homogenizer. Next, a PVK solution in tetrachloroethane was added to the dispersion and mixed, and the viscous mixture was ultrasonicated for 5 min. Polymer composites were prepared by casting a viscous solution of their components onto a transparent ITO electrode (In_2O_3:SnO_2) and dried for 3 h at 60°C. Films of the PVK–SWCNT composite were 10–20 μm in thickness.

In photocurrent measurements, a polymer layer was sandwiched between two electrodes, the transparent ITO electrode and the electrode that was made from a colloidal silver paste and had a diameter of about 3 mm. We measured the dark current j_d (before switching on light) and the kinetic curves of the total current buildup to a steady-state value j after switching on a laser at different values of the applied field E_0. The photocurrent was determined as the difference $j_{ph} = j - j_d$ after attaining a steady-state value of the total current. Nd:YAG and IS550-120 continuous wave laser systems radiating at 1064 and 1550 nm, respectively, were used.

The PR characteristics were measured in a cell shown in Figure 1 on a holographic device by the two-beam coupling technique using the linearly polarized radiation from a continuous Nd:YAG or IS550-120 laser. A linearly polarized laser beam was divided by a splitter into two beams of the same intensity of about $I_1(0) = I_2(0) = 0.14\ W/cm^2$ (Nd:YAG) and $I_1(0) = I_2(0) = 0.425\ W/cm^2$ (IS550-120). The polymer compositewas sandwiched between electrodes made from a transparent

conducting ITO film applied onto a glass substrate. To reduce the injection of holes from the anode, an Al_2O_3 film of a few nanometers in thickness was deposited on the ITO surface.

RESULTS AND DISCUSSION

As known, the optical-range of electronic absorption in SWCNT-based PR polymer composites extends to 2000 nm [5]. Figure 2 shows the field dependence of the quantum efficiency $\varphi(E)$ for the formation of mobile charge carriers in PVK–o-SWCNT (0.26 wt.%) exposed to the laser radiation with a wavelength of 1064 nm [Fig. 2 (1)] or 1550 nm [Fig. 2 (2)]. To determine the quantum efficiency, we measured the dependence of the photocurrent on the applied field $j_{ph}(E)$. The quantum efficiency was calculated by the equation

$$\varphi(E) = j_{ph}(E)hc/\{e\lambda[I_0(1 - 10^{(-A(\lambda))})]\},$$

where hc/λ is the photon energy at the wavelength of a laser, e is the electron charge, $I_0 = 5.2\,W/cm^2$ and $I_0 = 0.85\,W/cm^2$ are the intensities of Nd:YAG (1064 nm) and IS550-120 (1550 nm) lasers,

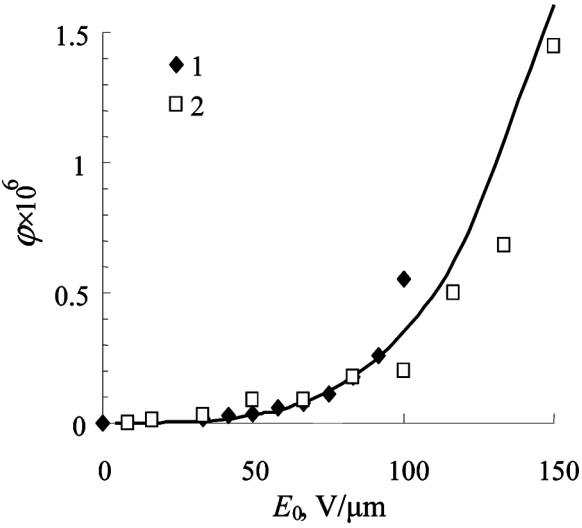

FIGURE 2 The electric field dependence of the quantum efficiency at (1) 1064 and (2) 1550 nm in PVK–o-SWCNT (0.26 wt.%). The solid line is constructed according to the Onsager equation $\psi = P(r_0E) \cdot \varphi_0$ calculated to within the fourth-power term $(E_0)^4$ ($\phi_0 = 0.012$ and $r_0 = 9.8$ Å)

respectively, $I_0(1 - 10^{(-A(\lambda)})$ is the light energy absorbed in the layer; and $A(\lambda)$ is the optical absorption at a wavelength λ [$A(\lambda) = \alpha d/2.3$, where α is the absorption coefficient and d is the layer thickness].

The solid line in Figure 2 is constructed according to the Onsager equation $\varphi = P(r_0, E_0) \cdot \varphi_0$ [6]. Here, $P(r_0, E_0)$ is the probability that the charges in a thermalized photogenerated electron-hole pair escape the recombination at the initial separation r_0. The value of $P(r_0, E_0)$ increases with both the initial charge separation distance in the pair r_0 and the applied field E_0. The probability was calculated to within the fourth-power term $(E_0)^4$. The calculated curve fits the experimental dependence at $r_0 = 9.8$ Å, and the quantum yield of pairs is $\varphi = 0.012$.

As was shown in Figure 2, the quantum efficiency in composite PVK–o-SWCNT at 1064 nm equals that at 1550 nm.

The PR effect was measured in composites PVK–o-SWCNT (0.26 wt.%), PVK–SWCNT (0.26 wt.%), and in these composites with the addition of 3 wt.% fullerene C_{60}. The use of both carbon nanotubes as a sensitizer and third-order nonlinear optical chromophores provides the PR sensitivity in the IR-region at 1064 and 1550 nm.

Figure 3 presents the two-beam coupling kinetic curves measured in the PVK composite containing 0.26 wt.% SWCNT (curve 1) and the composite which additionally contained 3 wt.% C_{60} (curves 2 and 3) with laser radiation at a wavelength of 1550 nm. The following sequence of operations was used for the measurement of the curves shown in Figure 3: beam 2 was first switched on, and its intensity at the exit from the cell $I_{2.0}$ was measured. Then, a negative potential was applied to the exit electrode; the intensity of beam 2 being not changed under these conditions. As is seen from the data in Figure 3, the intensity of beam 2, $I_{2.1}$, increased after switching on beam 1 (at the time $t = 10$ s). When beam 1 was switched off, the intensity of beam 2 acquired the initial value $I_{2.0}$. The gain in beam 2 is accompanied by a loss in the intensity of beam 1.

A relative rise in the intensity of beam 2 with time after switching on beam 1, $I_{2.1}$, can be represented by the expression

$$I_{2.1}/I_{2.0} = 1 + (\gamma_0 - 1)\{1 - \exp[-(t - t_0)/\tau]\}.$$

Here, γ_0 is the gain factor (or the intensity ratio $I_{2.1}/I_{2.0}$ under conditions, when $I_{2.1}$ reaches saturation), and τ is the diffraction grating formation time constant or the composite response time to the two-beam exposure.

The two-beam coupling gain coefficient Γ was calculated by the formula

$$\Gamma L = [\ln(\beta\gamma_0) - \ln(1 + \beta - \gamma_0)].$$

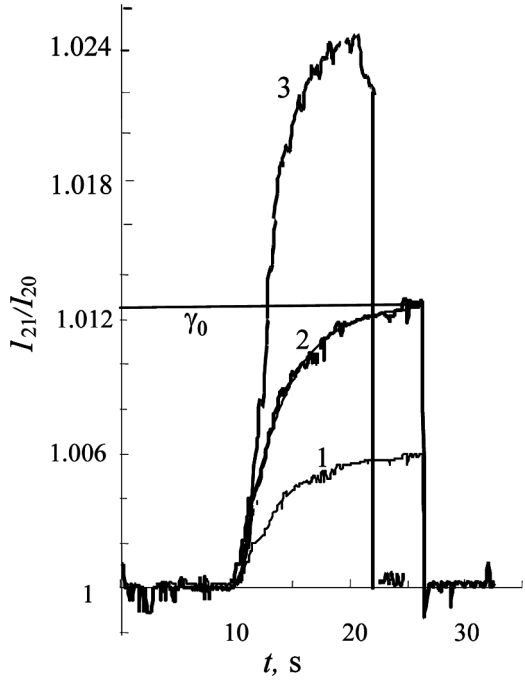

FIGURE 3 Two-beam coupling kinetic curves measured at 1550 nm (1) in composite PVK–SWCNT (0.26 wt.%), (2,3) - in composite PVK–SWCNT (0.26 wt.%) -C_{60}(3 wt.%), and (3)- in composite after its preliminary illumination for 1 min with a He-Ne laser (633 nm, $I = 0.06$ W/cm^2). A change in the intensity of beam 2 was measured in a field $E_0 = 40$ V/μm upon switching beam 1 on and off at a negative voltage on the exit electrode (Fig. 1).

Here, $\beta = I_1(0)/I_2(0) = 1$, $L = d/\cos(\phi - \theta)$ is the optical path length of beam 2, $(\phi - \theta) = 37.5^\circ$ is the angle between beam 2 and the normal to the layer surface (Fig. 1), and d is the layer thickness.

Figure 3 (curve 2) shows that the addition of C_{60} to the PVK–SWCNT composite leads to an almost double increase in the gain factor γ_0 for beam 2. It is likely that the effect is due to the strong acceptor properties of fullerene (the electron affinity is 2.66 eV [7]), namely, to the reduction in the distance over which electrons drift from their generation region (bright interference fringes) because of the scavenging by C_{60} molecules. This shortening leads to an increase in the phase shift ψ (Eq. 1) which is primarily determined by the range of holes before the trapping under these conditions. The possibility for Γ to grow due to the contribution of fullerene to the third-order bulk susceptibility cannot be ruled out as well [8].

Figure 3 (curve 3) shows a double increase in the gain factor γ_0 for beam 2 as a result of the 1-min preliminary illumination in the C_{60} absorption region (a He-Ne-laser, $\lambda = 633\,\text{nm}$, $I_0 = 0.06\ \text{W/cm}^2$) of composite PVK–SWCNT–C_{60} (in the absence of the field E_0). The increase in Γ can be associated with the filling of deep traps for holes during the preliminary illumination. This filling ensures both an increase of the distance, over which holes drift from their generation region and the increase in Γ as a result of the increase in the phase shift ψ [Eq. (1)].

So, the two-beam coupling gain coefficient Γ of a laser beam and the net gain Γ–α (difference of the gain and absorption coefficients) at $E_0 = 140$ V/cm are $32\,\text{cm}^{-1}$ and $27\,\text{cm}^{-1}$ in composite PVK–SWCNT–C_{60} ($\alpha = 4.6\,\text{cm}^{-1}$). The time constant τ decreases from ~ 4 to 0.9 s with an increase in E_0 from 33.3 to 140 V/μm. The preliminary illumination of this composite with a 633-nm laser beam (in the absence of the electric field) leads to an additional twofold increase in the two-beam coupling gain coefficient.

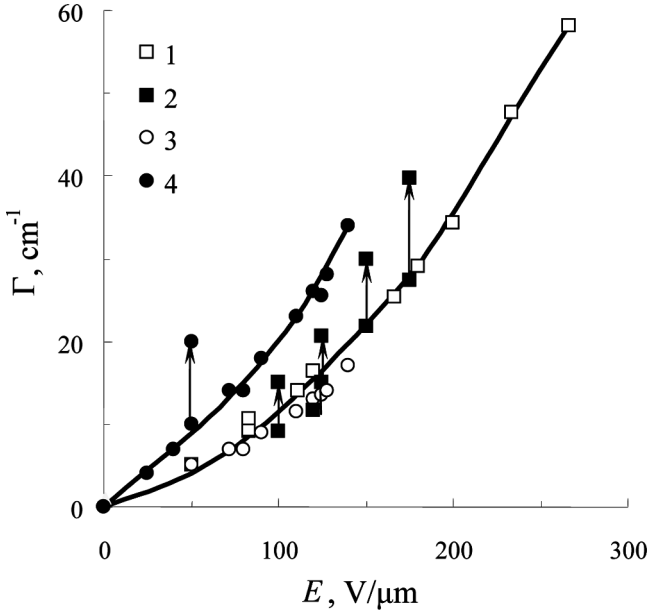

FIGURE 4 The field dependence of the two-beam coupling gain coefficient at 1550 nm in PVK–o-SWCNT (0.26 wt.%) (1,2) and PVK–SWCNT (0.26 wt.%) (3,4). (2,4); 3 wt.% C_{60} was added in the composites. Up arrow indicates that the measurement was made after the illumination for 1 min with a He-Ne laser (633 nm, $I = 0.06\ \text{W/cm}^2$) in composites with C_{60}.

Figure 4 shows the field dependences of the two-beam coupling gain coefficient with laser radiation at 1550 nm in the PVK composites containing 0.26 wt.% o-SWCNT (1,2) and (3,4) 0.26 wt.% SWCNT. It is worth to compare the effect of the additive of C_{60} on PR parameters of composites (Fig. 4, curves 2 and 4). As shown in Figure. 4 (curve 1,3), the field dependences of the two-beam coupling gain coefficient for both composites without C_{60} are the same. Figure 4 (curve 2) shows also that the two-beam coupling gain coefficient Γ is not changed with the addition of C_{60} into the composite containing o-SWCNT, but increases (curve 4) in composite PVK–SWCNT (due to the strong acceptor properties of C_{60}). It is clear that the attached oxygenous groups prevent the transfer of the electrons photogenerated in nanotubes on outside C_{60}. It is determined by an increase of the ionization potential of nanotubes after the oxidation.

Main PR-characteristics at 1064 nm in PVK–SWCNT 0.26 wt.% and in PVK–o-SWCNT 0.26 wt.% have higher values than those at 1550 nm. At the field $E_0 = 115$ V/μm, the net gain is $\Gamma\text{-}\alpha = 42\,\text{cm}^{-1}$ ($\alpha = 11\,\text{cm}^{-1}$) in PVK-SWCNT 0.26 wt.%. In composite PVK–o-SWCNT 0.26 wt.% at the field $E_0 =$ 170 V/μm, the net gain is $\Gamma\text{–}\alpha = 55\,\text{cm}^{-1}$ ($\alpha = 10\,\text{cm}^{-1}$).

Thus the single wall carbon nanotubes provide photorefractive properties at 1064 and 1550 nm of the composites based on PVK having high T_g (200°C), as these nanotubes have photoelectric sensitivity in the near IR region and a high third-order nonlinearity.

REFERENCES

[1] Moerner, W. E., Silence, S. M., Hache, F., & Bjorklund, G. C. (1994). *J. Opt. Soc. Am. B*, *11*, 320.
[2] Moerner, W. E. & Silence, S. M. (1994). *Chem. Rev.*, *94*, 127.
[3] Kippelen, B., Meerholz, K., & Peyghambarian, N. (1997). *Nonlinear Optics of Organic Molecules and Polymers*, CRC: Boca Raton.
[4] Ostroverkhova, O. & Moerner, W. E. (2004). *Chem. Rev.*, *104*, 3267.
[5] Licea-Jimenes, L., Grishina, A. D., Pereshivko, L. Ya., Krivenko, T. V., Savelyev, V. V., Rychwalski, R. W., & Vannikov A. V. (2006). *Carbon*, *44*, 113.
[6] Mozumder, A. (1974). *J. Chem. Phys.*, *60*, 4300.
[7] Sidorova, L. N., Yurovskaya, M. A., Borshchevskii, A. Ya., Trushkov, I. V., & Ioffe, I. N. (2005). *Fullerenes: Textbook*, Ekzamen: Moscow, (in Russian).
[8] Chen, Q., Kuang, L., Sargent, E. H., & Wang, Z. Y. (2003). *Appl. Phys. Lett.*, *83*, 2115.